Journal of Metals, Materials and Minerals, 34(3), 1955, 2024

Structural, morphological, magnetic, and dielectric properties of copper-substituted $Cu_XZn_{(1-X)}Fe_2O_4$ nanoparticles: Green synthesis

Gavisiddaiah HARISHA[1,2], Ramakrishnaiah THEJAS[3], B Venkatagiriyappa PADMINI[4], Chinnappa Reddy DEVARAJA[5,*], Malalkere Veerappa MURUGENDRAPPA[6], and Koppa Mahadevappa RAJASHEKARA[1,*]

[1] *Department of Physics, S J C Institute of Technology, Chikkaballapura, Karnataka 562101 India*
[2] *Visvesvaraya Technological University, Belagavi, Karnataka 590018, India*
[3] *Department of Physics, The National College, Jayanagar, Bengaluru, Karnataka 560070, India*
[4] *Department of Mechanical Engineering, Sambram Institute of Technology, Bangalore, Karnataka 560100, India*
[5] *Department of Physics, Manipal Institute of Technology Bengaluru, Manipal Academyof Higher Education, Manipal, Karnataka 576104, India*
[6] *Department of Physics, B.M.S. College of Engineering, Bengaluru, Karnataka 560019,India*

***Corresponding author e-mail**: devaraja.c@manipal.com, km_rajashekar@yahoo.co.in

Received date:
3 February 2024
Revised date:
17 April 2024
Accepted date:
11 June 2024

Keywords:
XRD;
SEM;
TEM;
Magnetic properties;
Dielectric studies

Abstract

Structural, Magnetic, and Dielectric investigations on the "CuX Zn(1-X) Fe_2O_4" X with stoichiometry (X=0, 0.3, 0.5, 0.7, and 1) were synthesized by solution combustion method using Aloe Vera extraction. The X-ray diffraction method was utilized to characterize the as-synthesized Cu-Zn ferrites. The results indicated the presence of cubic spinel structure with $Fd^{-3}m$ space group, and absence of other contaminates. The lattice parameter was found to increase with the increase in Zinc concentration. The patterns of TEM confirm that the particle is within the nanometer range (35 nm to 50 nm). Magnetic properties investigated by vibrating sample magnetometry, reveal that the MS, MR, and HC values decrease with an increase in Zn concentration. The dielectric studies performed at room temperature show that the increase in frequency decreased the dielectric loss and $Cu_{0.5}Zn_{0.5}Fe_2O_4$ exhibits higher dielectric constant and dielectric loss are studied at the frequency range studied. Thus, the prepared samples have potential applications in semi-conductor and EMI shielding devices.

1. Introduction

Ferrites have wide applications in areas viz inductors, transformers, refrigerator magnets, microwaves, etc, owing to their low eddy current losses [1,2]. They possess cubic spinel structures having a general formula AB_2O_4, where A is any divalent metal like Mn^{2+}, Cu^{2+}, Ni^{2+}, Zn^{2+}, and B denotes a trivalent material like Cr^{3+}, Fe^{3+}. Ferrites reveal outstanding structural, magnetic, and electrical properties [3]. Amid numerous ferrites, Cu–ferrites exhibit a polycrystalline nature associated with high dielectric constant, the properties of which are highly dependent on the size of the crystals, preparation method, and type of elements that substitute it [4]. Several methods like hydrothermal [5], chemical co-ppt [6], sol-gel [7,8] combustion, conventional ceramic process, RF sputtering [9-13], and auto combustions [14] are utilized to synthesize nano ferrites. The spinel-structured ferrites have also made their impact in applications like magnetic storage systems, spintronics, and magnetic resonance [15-17] due to their exceptional magnetic properties. Several investigations have been made to incorporate the substitutional effects of $CuFe_2O_4$ on the structural, electrical, and magnetic properties. $ZnFe_2O_4$ is being synthesized for the study, and its photocatalytic activity in degrading organic dyes under visible light is being examined [18]. S. G Doh *et al.* have reported that $Ni_{1-X}Cu_X$ Fe_2O_4 powders, synthesized by Co-ppt, exhibit the highest magnetization at X=0.5 [19]. The same powder, synthesized by ceramic method, has been reported to increase coercive field, with a decrease in grain size [20]. The investigation by A R Lamani *et al.* on $Cu_{1-X}Zn_XFe_2O_4$ shows an increase in dielectric constant and loss tangent [21] with an increase in Zn concentration. A C Murrieta *et al.* study delves into the characterization of $ZnFe_2O_4$ spinel ferrite synthesized through hydrothermal methods, providing insights into the microstructure, inversion degree, and crystal evolution [22]. The substitution of Ga in $Cu_{0.5}$ $Zn_{0.5}$ $Fe_{2X}Ga_XO_4$ is found to decrease the transition temperature with its increase and elucidates the semiconducting behavior [23]. Aloe vera is a cactus a plant, that grows in hot and dry climates, [24] and it is recently reported that it can be used for successful synthesis of gold and silver nanoparticles of 50 nm to 350 nm and 15 nm respectively [25]. Santi Phumying *et al.*, have reported its use in the synthesis of indium oxide and various other complex oxide nanoparticles [26]. N. Matinise *et al.*, present a paper detailing the environmentally friendly synthesis of nanocomposites comprised of mixed-phase bismuth ferrite oxide ($BiFeO_3$). This study assesses the viability of these composites as effective electrode materials for applications in supercapacitors [27]. N. T. Nguyen *et al.* focused on the environmentally friendly synthesis of $ZnFe_2O_4$@ZnO nano-

composites utilizing floral waste from Chrysanthemum spp and here the nanocomposites are explored for their efficacy in photocatalytic dye degradation [28]. The aloe vera gel, which was once used in cosmetics, anti-inflammatory, and burn treatments, is now being used as a good reducing agent to produce nanoparticles. Green synthesis of nano Cu ferrites using aloe vera offers numerous advantages, including environmental friendliness, biocompatibility, cost-effectiveness, facile synthesis routes, controlled morphology and properties, energy efficiency, and scalability. These benefits underscore the importance of adopting green synthesis approaches in nanotechnology for sustainable development and technological advancement. In the present investigation, a novel solution combustion method has been used to synthesize $Cu_XZn_{(1-X)}Fe_2O_4$ (Cu-Zn ferrites) in the presence of the aloe vera plant extract as fuel. the structural morphology, dielectric, and magnetic properties of the Cu-substituted Zn ferrites are studied and reported.

2. Experimental methods

The nanocrystalline $Cu_XZn_{1-X}Fe_2O_4$ (X=0, 0.3, 0.5, 0.7, and 1) were prepared by solution combustion technique using Aloe vera gel as the oxide fuel. The molar stoichiometric amounts of metal nitrates ($Zn(NO_3)_2{\cdot}6H_2O$, $Cu(NO_3)_2{\cdot}3H_2O$ and $Fe(NO_3){\cdot}9H_2O$), were combined with 10 mL of Aloe vera gel. This gel was extracted from the pulp of its leaf and purified with a muslin cloth. The resultant metal nitrate and fuel were diluted with 50 mL of distilled water and mixed thoroughly in a magnetic stirrer for 45 min to get a homogenous solution. This solution was taken in a borosilicate glass and kept in a muffle furnace which was preheated and maintained at 450°C. The powder thus obtained was crushed in a mortar, and calcined at 800°C for 1 h to remove any contaminates. The phases and crystal structure of the powder were identified by XRD (X-Ray diffraction Bruker AXS D8 advance) containing Cu Kα- wavelength of 1.54 Å. The morphology of the powders along with their particle size were characterized by SEM (Scanning Electron Microscopy with EDAX JEOL 6390) and crystallinity was visualized by TEM (Transmission Electron Microscope, Hitachi H-7500). The room temperature magnetic and dielectric properties were examined by VSM (vibrating sample Magnetometer, Lake Shore 7400) and impendence analyzer (Wayne Kerr 6500 B) respectively. The materials were procured from a local vendor, M/s Vasa Scientific Centre Bangalore, synthesis of nano ferrite.

Chemical reaction:

$Zn(No_3)2.6H_2O$ (aq) + $Cu(NO_3)_2 3H_2O$ (aq) + $C_{19}H_{28}O_{14}$/aloe vera plant extract (aq) → $Cu_xZn_{1-x}Fe_2O_4$ (s) + $36H_2O$ (g) + $12N_2$ (g) + $8CO_2$ (g)

3. Results and discussion

3.1 Structural details

The X-ray diffraction motifs of the $Cu_XZn_{(1-X)}Fe_2O_4$ samples of compositions X=0, 0.3, 0.5, 0.7, and 1, are shown in Figure 1. It can be observed from the X-ray diffraction patterns that, all the samples display a single-phase structure, with the absence of impurities within the range of XRD.

This indicates that the process employed for synthesis is successful in producing high-purity final products. The principal peaks obtained correspond to a characteristic planar spacing found between (220), (311), (400), (422), (511), and (440), which matches the JCPDS data 901-2438 and confirms the formation of spinel Copper ferrite and Zinc ferrites (JCPDS 22-1012). The average size of the crystals was calculated using Debye – Scherer's Equation (1).

$$D_{hkl} = 0.94\lambda/\beta\cos\theta \quad (1)$$

Where λ = X-ray wavelength equal to 1.5406 A˚,

θ = Bragg diffraction angle,

β (radians) = full width at half maximum.

The lattice constants were determined by extrapolating from the most glaring peaks [28-30] using the Equation (2).

$$a = \frac{(h^2+k^2+l^2)^{\frac{1}{2}}}{2sin\theta} \quad (2)$$

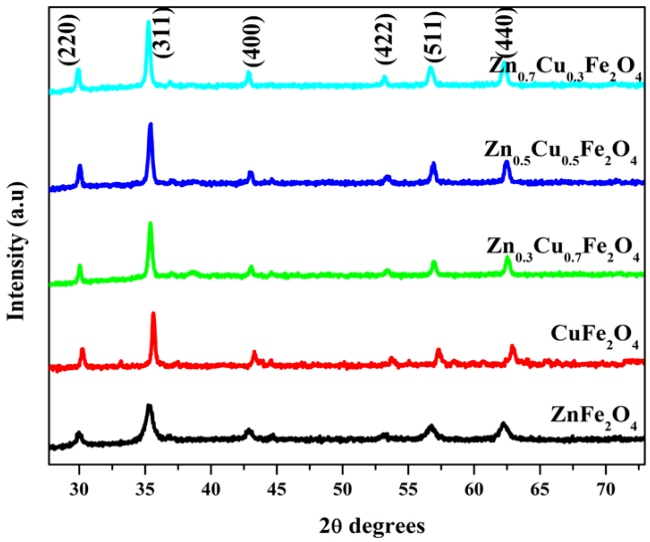

Figure 1. XRD peaks of $Cu_xZn_{1-x}Fe_2O_4$ (X=0, 0.3, 0.5, 0.7, 1) nanoparticles.

Table 1. Rietveld refinement parameter from the PXRD data for $Cu_xZn_{1-x}Fe_2O_4$ (X=0, 0.3, 0.5, 0.7, and 1).

Compound name	Crystal system	Crystal system	Crystallite size (nm)	Parameter (A^0)		R – factors			
				a=b=c	Cell volume ($A^{0\,3}$)	R_p	R_{wp}	GOF(χ^2)	R_{exp}
$ZnFe_2O_4$	$Fd^{-3}m$	Spinal cubic	14.35	8.44	601.73	1.78	2.27	1.23	1.84
$Zn_{0.7}Cu_{0.3}Fe_2O_4$	$Fd^{-3}m$	Spinal cubic	33.87	8.42	597.68	1.69	2.11	1.11	1.91
$Zn_{0.5}Cu_{0.5}Fe_2O_4$	$Fd^{-3}m$	Spinal cubic	34.94	8.40	594.43	2.18	2.78	1.45	1.92
$Zn_{0.3}Cu_{0.7}Fe_2O_4$	$Fd^{-3}m$	Spinal cubic	37.28	8.39	591.08	2.19	2.77	1.38	2.00
$CuFe_2O_4$	$Fd^{-3}m$	Spinal cubic	46.25	8.34	580.48	2.05	2.58	1.48	1.75

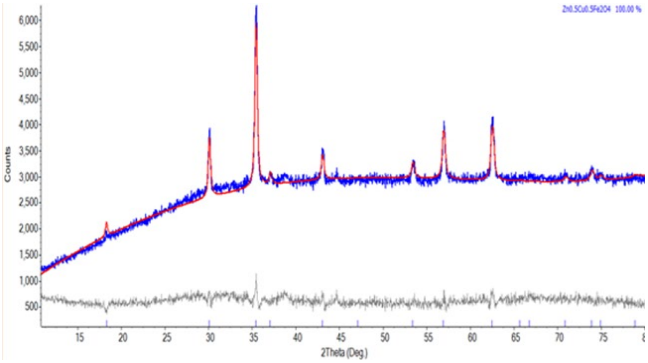

Figure 2. Rietveld refinement plot of $Zn_{0.5}Cu_{0.5}Fe_2O_4$.

Further analysis was accomplished based on the Rietveld refinement method, using TOPAS 6 software. Figure 2 shows the refinements plots and reliability factors R_p, R_{wp} along with goodness of fit. The average particle size, as estimated by the Deby-Scherrer equation [28-30] is found to be in the range of 14 nm to 46 nm. The size comparisons shown in Table 1 are used to assess the crystallinity of nanoparticles. The samples show excellent crystalline sizes with particle sizes in the nanoscale range. It can be observed that the crystal size increases with an increase in Cu content and is due to the influence of Cu on the crystal structure of ferrite. Copper has a large ionic radius in comparison to the ferrites (Fe, Zn) and can be confirmed by the shift in the diffraction peak towards the lower angle. This may be explained based on Vegard's law [31]. The results of XRD reveal that nano-crystalline powders at room temperature synthesized utilizing Aloe vera plant extraction act like a complexing agent to chelate metal cations and mix them homogenously on an atomic scale.

3.2 Morphology and microstructure

The morphology of the samples was investigated by Scanning Electron Microscope and is shown in Figure 3. The SEM images depict a spherical shape with dense structures and porosity located at agglomerated linkages. The average grain size was found to be in the range of 40 nm to 50 nm and is in good agreement with the estimated XRD data analysis. The analysis of the composition, examined under EDAX (Energy dispersive analysis spectrum) is displayed in Figure 4.

The spectra confirm the presence of O, Fe, Cu, and Zn, employed in synthesis, and are close to the stoichiometric value. Transmission Electron Microscope (TEM) was utilized to obtain high-resolution images [29,30]. Figure 5 reveals the detailed structures of the samples. The images confirm a spherical shape with evident agglomerations Patchy circular rings without any diffraction spots, along with secondary phase rings, reveal a crystalline spinel structure.

3.3 Magnetic properties

The field dependence M-H curve (magnetic – hysteresis curves) of the specimens examined at ambient temperature as measured by VSM at an applied field at room temperature [–20KOe < H < 20KOe] are shown in Figure 6. The hysteresis loops show a ferromagnetic effect on the magnetic properties with the substitution of Cu. and the synthesized material was found to be soft magnetic material [28]. From Table 2 it can be observed that Ms (saturation magnetization) M_R (Retentivity) and Hc (coercivity) tend to decrease with an increase in Cu content. This agrees with the results of V. Angadi *et al.* [32],

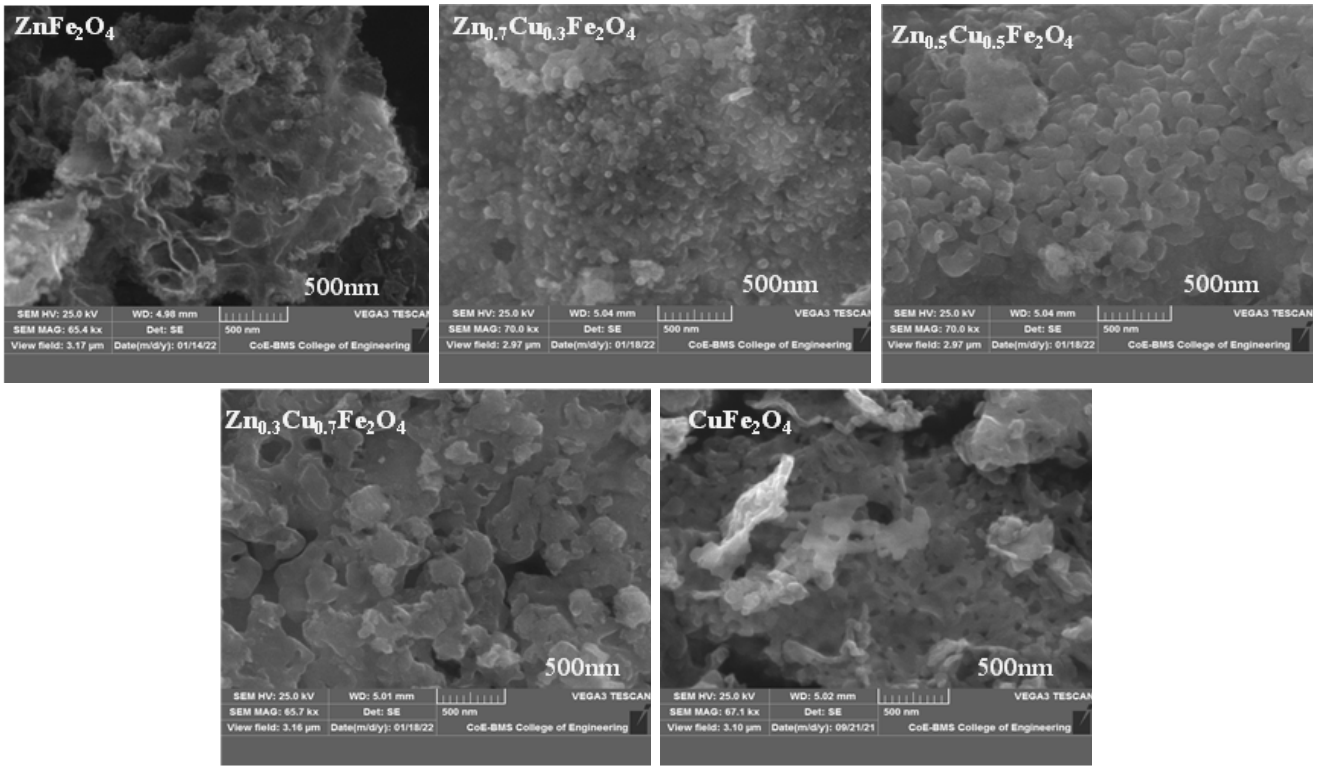

Figure 3. SEM images of $Cu_xZn_{1-x}Fe_2O_4$ (X=0, 0.3, 0.5, 0.7, 1) nanoparticles.

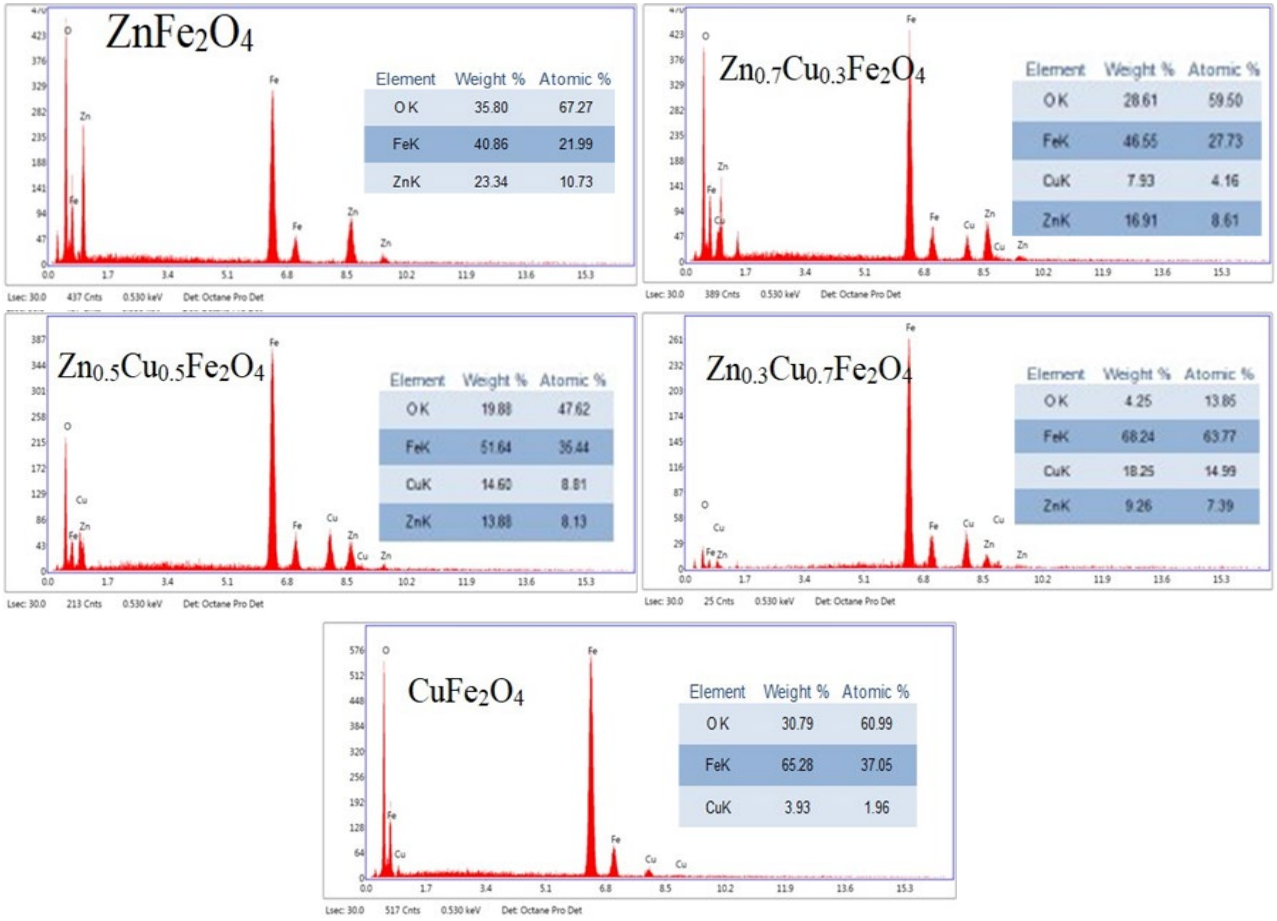

Figure 4. EDAX spectra of CuxZn1-xFe2O4 (X=0, 0.3, 0.5, 0.7, nanoparticles.

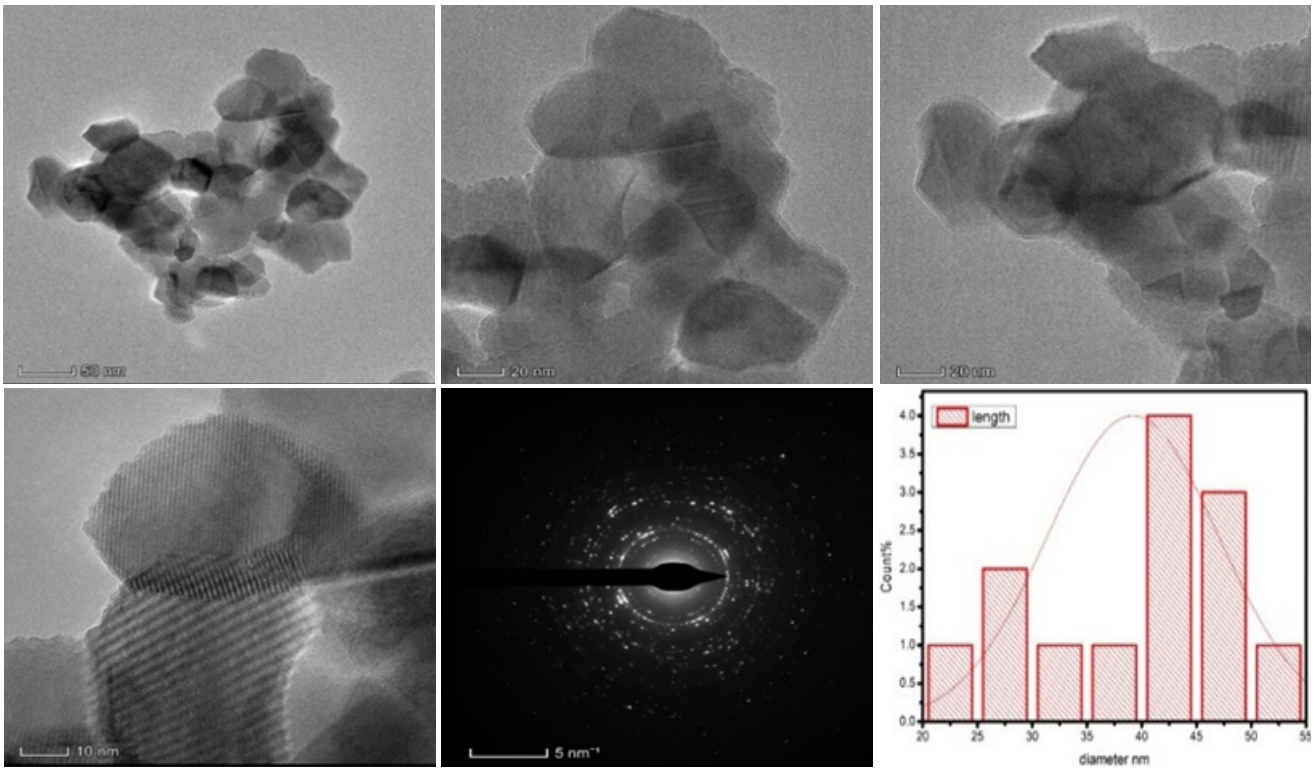

Figure 5. TEM images of $Cu_{0.5}Zn_{0.5}Fe_2O_4$ nanoparticles.

Table 2. Coercivity, Retentivity, Saturation level of CuxZn1-xFe2O4 (X=0, 0.3, 0.5, 0.7, and 1) nanoparticles.

Composition	Lattice parameters (A0)	Crystallite size (nm)	Coercivity (HC) (Oe)	Retentivity (MR) ($emu \cdot g^{-1}$)	Saturation level MS ($emu \cdot g^{-1}$)
$ZnFe_2O_4$	8.44	14.35	148.557	14	52.66
$Zn_{0.7}Cu_{0.3}Fe_2O_4$	8.42	33.87	118.99	8.10	40.2
$Zn_{0.5}Cu_{0.5}Fe_2O_4$	8.40	34.94	90.84	6.415	40.75
$Zn_{0.3}Cu_{0.7}Fe_2O_4$	8.39	37.28	47.6133	2.130	26.51
$CuFe_2O_4$	8.34	46.25	112.535	0.3465	4.1

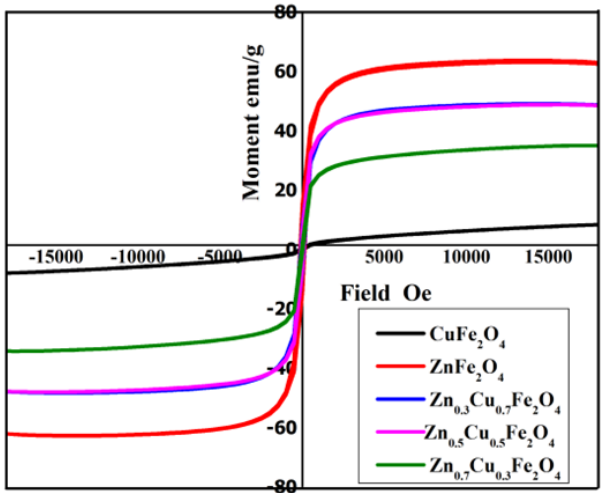

Figure 6. M-H loop of $Cu_xZn_{1-x}Fe_2O_4$ (X=0, 0.3, 0.5, 0.7, 1) nanoparticles.

where the M_s, M_r, and H_c values decrease with an increase in Zn concentration. The decrease in the coercivity values, as Cu increases, may be due to lower magnetic moment [33] and the possible substitution for Cu for other elements may alter the distribution of magnetic moments. The net moments as given by Neel's model given by μ^{th} =MB(x)-MA(x), where A and B are sub-lattice magnetic moments [34]. The decline in magnetization [35] may also be attributed to the surface effects, surface spins, and the existence of the glassy state. With the increase in $CuFe^{3+}$ ions migrate from B to A site and Zn^{2+} concentration decreases from both AA sites. It is well established that the Hc value decreases with an increase in grain size. In the present study, low coercive values are obtained leading to the probability of lower domain rotation. Materials with increased grain size are used in applications involving lower core loss [36]. Coercive force and domain rotation in ferrites can be obtained by reversing the wall movement direction and the direction of the applied magnetic field, respectively. The saturation levels obtained range from 4.1 to 52.66 and are found to decrease with an increase in Cu levels. The decrease in saturation values with an increase in Cu levels for $Cu_X\ Zn_{(1-X)}\ Fe_2O_4$ nanoparticles can be attributed to the introduction of Cu ions, which disrupt the magnetic ordering of the spinel structure, leading to a decrease in the overall magnetic moment per formula unit. This phenomenon is justified by the dilution of Fe ions' magnetic moments by non-magnetic Cu ions, thereby reducing the overall saturation magnetization of the nanoparticles The magnetic properties of spinel ferrites are influenced by shape, size, crystallinity magnetic direction and are very much dependent on its preparation method [28].

3.4 Dielectric properties

The dielectric properties of all the samples were studied at room temperature by an impedance analyzer (Wayne Kerr 6500B). The variation of dielectric constant with frequency is shown in Figure 7(a) and exhibits inverse proportionality a typical behavior of spinel ferrites [37]. This phenomenon for increased dielectric constant with a decrease in frequency is by Koops and can be attributed to the conducting grains with insulating grain boundaries [38,39] and is well explained by space charge polarization, where the non-ferro electric regions, surround the ferroelectric regions [40].

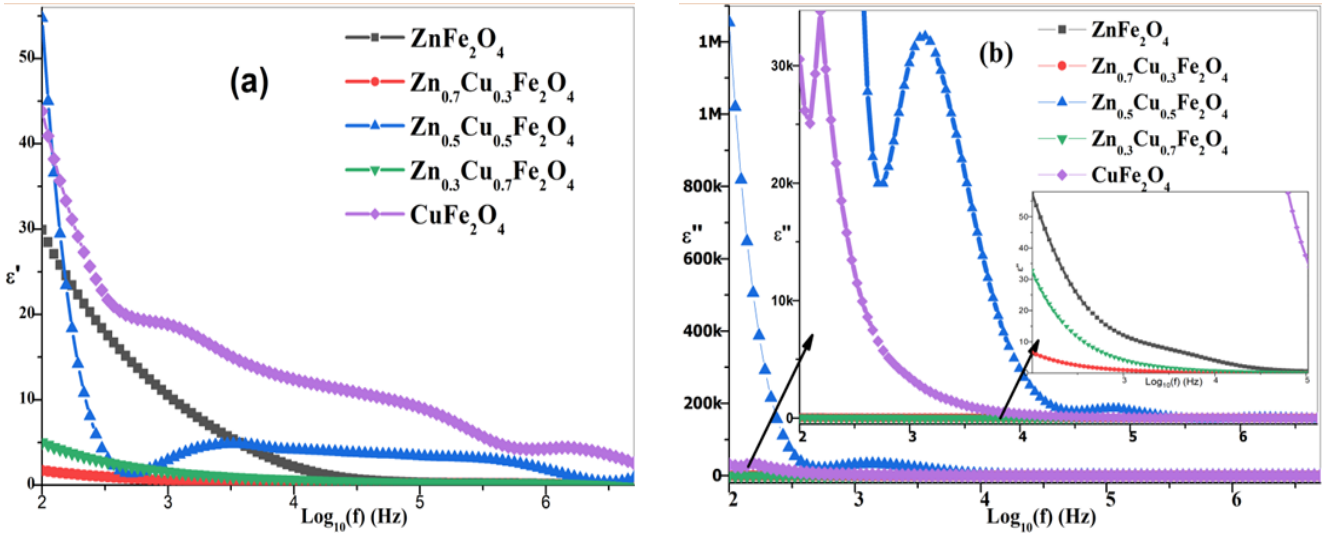

Figure 7. (a) Dielectric constant real, and (b) Dielectric constant imaginary of $Cu_xZn_{1-x}Fe_2O_4$ (X=0, 0.3, 0.5, 0.7, 1) nanoparticles.

Figure 7(b) represents the variation of dielectric loss, concerning frequency. It can be seen that a similar trend (increase in frequency, decrease in dielectric loss) persists. $Zn_{0.5}Cu_{0.5}Fe_2O_4$ exhibits higher dielectric constant (also loss) and $Zn_{0.7}Cu_{0.35}Fe_2O_4$ shows that lower value, among the studied samples and the reason may be due to the replacement of ferrous ions and its occupancy, at octahedral positions [41].

4. Conclusion

The principal motivation for the current research is to examine the structural, morphological, magnetic, and dielectric characteristics of Cu substituted Zn nano ferrites, synthesized by a novel method of green synthesis (Aloe vera gel extract), in the range of (0, 0.3, 0.5, 0.7, and 1). The XRD motif showed that the compounds obtained were spinel cubic structures with $Fd^{-3}m$ spacings. The increased substitution of Zn for Cu is responsible for the increased crystalline size and the sample size between 40 nm to 50 nm SEM and TEM were utilized to find the surface morphology and the analysis confirmed the presence of spherical shape with 20 nm to 50 nm crystal size. EDAX analysis confirms purity and uniformity and TEM confirms the presence of secondary phase rings with spinel structures. The magnetic properties analyzed, clearly indicate the impact of crystal size on Coercivity and saturation. Magnetization and Retentivity. The investigation on dielectric properties shows that Cu has a larger ε' value and that the synthesized material is a prospective applicant in microwave and electrical devices applications.

References

[1] A. Azam. "Microwave-assisted synthesis and characterization of Co doped Cu ferrite nanoparticles," *Journal of alloys and compounds*, vol. 540, pp. 145-153, 2012.

[2] S. Tao, F. Gao, X. Liu, and O. T. Sørensen. "Preparation and gas-sensing properties of $CuFe_2O_4$ at reduced temperature," *Materials Science and Engineering: B,* vol. 77, no.2 , pp.172-176, 2000.

[3] H. Sozeri, H. Deligoz, H. Kavas, and A. Baykal, "Magnetic, dielectric and microwave properties of M–Ti substituted barium hexaferrites (M= Mn^{2+}, Co^{2+}, Cu^{2+}, Ni^{2+}, Zn^{2+})", *Ceramics International*, vol. 40, pp. 8645-8657, 2014.

[4] V. Manikandan, A.Vanitha, E. R. Kumar, and J. Chandrasekaran, "Effect of sintering temperature on structural and dielectric properties of Sn substituted $CuFe_2O_4$ Nanoparticles," *Journal of Magnetism and Magnetic Materials*, vol. 423, pp. 250-255, 2017.

[5] T. Koutzarova, S. Kolev, C. Ghelev, K. Grigorov, and I. Nedkov, "Structural and magnetic properties and preparation techniques of nano-sized M-type hexaferrite powders," *Advances in Nanoscale magnetism*, vol. 1, pp. 183-203, 2009.

[6] S. S. Khot, N. S. Shinde, B. P. Ladgaonkar, B. Bkale, and S. C. Watawe, "Magnetic and structural properties of magnesium zinc ferrites synthesized at different temperature" *Advances in Applied science research*, vol. 2, pp. 460-471, 2011.

[7] V. Pillai, P. Kumar, M. S Multani, and D. O Shah, "Structure and magnetic properties of nanoparticles barium ferrite synthesized using micro emulsion processing," *colloids and surfaces A: physicochemical and engineering Aspects,* vol. 80, pp. 69-75, 1993.

[8] L. Lechevallier, J. M. Le Breton, J. F.Wang, and I. R. Harris, "Structural analysis of hydrothermally synthesized $Sr_{(1-x)}Sm_xFe_{12}O_{19}$ hexagonal ferrites," *Journal for magnetism and magnetic materials*. vol. 269, pp. 192-196, 2004.

[9] C. O. Augustin, R. kalaiselvan, R. Nagaraj, and L. John Berchmans, "Effect of La^{3+} substitution on the structural, electrical and electrochemical properties of strontium ferrite by citrate combustion method," *Materials Chemistry and Physics*, vol. 89, pp. 406-411, 2005.

[10] K. C. Patil, S. T. Aruna, and S. Ekambrarm, "Combustion synthesis, *Current opinion in solid state and materials science*, vol. 2, pp. 158-165, 1997.

[11] E. Wu. S. J Campbell, and W. A Kaczmarek, "Mossbauer effect study of ball- milled strontium ferrite, *Journal of magnetism and magnetic materials*, vol. 177, pp. 255-256, 1998.

[12] W. A Kaczmarek, B. IdZikowski, and K. H Muller, "XRD and VSM study of ball milled $SrFe_{12}O_{19}$ powder "*Journal of magnetism and magnetic materials*, vol. 177, pp. 921-922, 1998.

[13] A. Sharma, O. Modi, and G. Gupta, "Effect of fuel to oxidizer ration a synthesis of alumina powder using solution combustion technique – aluminium nitrate and glycine combination," *Advances in Applied science Research*, vol. 3, pp. 2151-2158, 2012.

[14] T. Liu, L. Wang, P. Yang, and B. Hu, "Preparation of nanometer $CuFe_2O_4$ by auto combustion and its catalytic activity on the thermal decomposition of ammonium perchlorate," *Materials Letters*, vol. 62, pp. 4056-4058, 2008.

[15] D. H Han, H. L Luo, and Z. Yang. "Remanent and anisotropic switching field distribution of platelike Ba-ferrite and acicular particulate recording media," *Journal of magnetism and magnetic materials*, vol. 161, pp. 376-378, 1996.

[16] P. Seneor, A. Fert, J. L. Maurice, F.Montaigne, F. Petroff, and A. Vaures. "Large magnetoresistance in tunnel junctions with an iron oxide electrode," *Applied Physics Letters*, vol. 74, no. 26, pp. 4017-4019, 1999.

[17] G. Hu, and Y. Suzuki. "Negative Spin Polarization of Fe_3O_4 in Magnetite/Manganite-Based Junctions," *Physical review letters*, vol. 89, no. 27, p. 276601, 2002.

[18] T. P. Oliveira, G. N. Marques, M. A. Castro, R. C. Costa, J. H. Rangel, S. F. Rodrigues, C. C. dos Santos, and M. M. Oliveira. "Synthesis and photocatalytic investigation of $ZnFe_2O_4$ in the degradation of organic dyes under visible light," *Journal of Materials Research and Technology*, vol. 9, no. 6, pp. 15001-15015, 2020.

[19] S. G. Doh, E. B. Kim, B. H. Lee, and J. H. Oh. "Characteristics and synthesis of Cu–Ni ferrite nanopowders by coprecipitation method with ultrasound irradiation," *Journal of Magnetism and Magnetic Materials*, vol. 272, pp. 2238-2240, 2004.

[20] J. Msomi, and T. Moyo. "Effect of domain transformation on the magnetic properties of $Cu_xNi_{1-x}Fe_2O_4$ ferrites," *Journal of magnetism and magnetic materials,* vol. 321, no. 9, pp. 1246-1250, 2009.

[21] A. R. Lamani, H. S. Jayanna, P. Parameswara, R. Somashekar, R. Rao, and G. D. Prasanna. "Dielectric properties of poly-

crystalline Cu–Zn ferrites at microwave frequencies," *Journal of Alloys and Compounds,* vol. 509, no. 18, pp. 5692-5695, 2011.

[22] A. C Murrieta, D Cavazos-Cavazos, C Flores-Jauregui, P Sepulveda, M Hesiquio-Garduño, and F. F. Contreras-Torres. "Characterization of hydrothermally synthesized $ZnFe_2O_4$ spinel ferrite: Insights into microstructure, inversion degree, and crystal evolution," *Journal of Physics and Chemistry of Solids*, vol. 183, p. 111659, 2023.

[23] S. S. Ata-Allah. "Influence of Ga substitution on the magnetic and electric behaviour of $Cu_{0.5}Zn_{0.5}Fe_2O_4$ compound," *Journal of magnetism and magnetic materials*, vol. 284, pp. 227-238, 2004.

[24] S. Choi, and M. H. Chung. "A review on the relationship between Aloe vera components and their biologic effects," *In Seminars in integrative medicine WB Saunders*, vol. 11, no. 1, pp. 53-62, 2003.

[25] S. P. Chandran, M. Chaudhary, R. Pasricha, A. Ahmad, and M. Sastry, "Synthesis of gold nanotriangles and silver nanoparticles using Aloevera plant extract," *Biotechnology progress*, vol. 22, no. 2, pp. 577-583, 2006.

[26] S. Phumying, S. Labuayai, E. Swatsitang, V. Amornkitbamrung, and S. Maensiri. "Nanocrystalline spinel ferrite (MFe_2O_4, M= Ni, Co, Mn, Mg, Zn) powders prepared by a simple aloe vera plant-extracted solution hydrothermal route," *Materials Research Bulletin*, vol. 48, no. 6, pp. 2060-2065, 2013.

[27] N. Matinise, N. Botha, and IG M M. Maaza. "Mixed-phase bismuth ferrite oxide ($BiFeO_3$) nanocomposites by green approach as an efficient electrode material for supercapacitor application," *MRS Advances*. pp. 1-5, 2023.

[28] N. T. Nguyen, L. M. Nguyen, T. T. Nguyen, N. H. Nguyen, D. H. Nguyen, D. T. Nguyen, and T. Van Tran. "Green synthesis of $ZnFe_2O_4$@ ZnO nanocomposites using Chrysanthemum spp. floral waste for photocatalytic dye degradation," *Journal of Environmental Management*, vol. 326, p. 116746, 2023.

[29] Anuj Jain, Ravi Kant Baranwal, Z. Ajaya Bharti,Vakil, and C. S. Prajapati, "Study of Zn-Cu ferrite nanoparticles for LPG Sensing," *Hindawi Publishing Corporation the Scientific World Journal,* pp. 1-7, 2013.

[30] A. Mahmood, and A. Maqsood, "Physical properties, magnetic measurements, dielectric relaxation, and complex impedance studies of cobalt-doped zinc ferrite nanoparticles," *Applied Nanoscience,* vol. 11, pp. 2311-2336, 2021.

[31] A. R. Denton, and N. W. Ashcroft. "Vegard's law," *Physical review A*, vol. 43, no. 6, p. 3161, 1991.

[32] V. J. Angadi, B. Rudraswamy, K. Sadhana, and K. Praveena, "Structural and magnetic properties of manganese zinc ferrite nanoparticles prepared by solution combustion method using mixture of fuels," *Journal of Magnetism and Magnetic Materials*, vol. 409, pp. 111-115, 2016.

[33] R. Pena-Garcia, A. Delgado, Y. Guerra, G. Duarte, L. A. Gonçalves, and E. Padron-Hernandez, "The synthesis of single-phase yttrium iron garnet doped zinc and some structural and magnetic properties," *Materials Research Express*, vol. 4, p. 016103, 2017.

[34] L. Néel. "Antiferromagnetism and ferrimagnetism," *Proceedings of the Physical Society. Section*, vol. 65, no. 11, p. 869, 1952.

[35] M. G. Del Muro, X. Batlle, and A. Labarta. "Erasing the glassy state in magnetic fine particles," *Physical Review B*," vol. 59, no. 21, p. 13584, 1999.

[36] P. Yaseneva, M. Bowker, and G. Hutchings. "Structural and magnetic properties of Zn-substituted cobalt ferrites prepared by co-precipitation method," *Physical Chemistry Chemical Physics,* vol.13, no.41, pp.18609-18614 2011.

[37] A. A. Sattar, and S. A. Rahman. "Dielectric properties of rare earth substituted Cu–Zn ferrites," *physica status solidi (a)*, vol. 200, no. 2, pp. 415-422, 2003.

[38] C. G.Koops. "On the dispersion of resistivity and dielectric constant of some semiconductors at audio frequencies," *Physical review*, vol. 83, no. 1, p. 121, 1951.

[39] S. Upadhyay, D. Kumar, and O. M. Parkash. "Effect of composition on dielectric and electrical properties of the $Sr_{1-x}La_xTi_{1-x}Co_xO_3$ system," *Bulletin of Materials Science*, pp. 513-525, 1996.

[40] E. R. Kumar, T. Arunkumar, and T. Prakash. "Heat treatment effects on structural and dielectric properties of Mn substituted $CuFe_2O_4$ and $ZnFe_2O_4$ nanoparticles," *Superlattices and Microstructures*, vol. 85, pp. 530-535, 2015.

[41] H. Sozeri, H. Deligoz, H. Kavas, and A. Baykal, "Magnetic, dielectric and microwave properties of M–Ti substituted barium hexaferrites (M= Mn^{2+}, Co^{2+}, Cu^{2+}, Ni^{2+}, Zn^{2+})," *Ceramics International*, vol. 40, pp. 8645-8657, 2014.